A White Light Interferometer for Improved Achromatic Holographic Lithography

by

Satyen N. Shah

Submitted to the Department of Electrical Engineering and Computer Science
in partial fulfillment of the requirements for the degree of

Bachelor of Science in Electrical Science and Engineering

at the

MASSACHUSETTS INSTITUTE OF TECHNOLOGY

May 1993

Author .....
Department of Electrical Engineering and Computer Science
May 18, 1993

Certified by .....
Henry I. Smith
Joseph F. and Nancy P. Keithley Professor of Electrical Engineering
Thesis Supervisor

Accepted by .....
Leonard A. Gould
Chairman, Departmental Committee on Undergraduate Students

A White Light Interferometer for Improved Achromatic Holographic Lithography

by

Satyen N. Shah

Submitted to the Department of Electrical Engineering and Computer Science
on May 17, 1993, in partial fulfillment of the
requirements for the degree of
Bachelor of Science in Electrical Science and Engineering

Abstract

In this thesis, I refined and improved an implementation of achromatic holographic lithography which is a method of producing fine period gratings over large areas. One major improvement to the system was the creation of a white light interferometer for the purpose of bringing the system within the depth of focus.

Thesis Supervisor: Henry I. Smith
Title: Joseph F. and Nancy P. Keithley Professor of Electrical Engineering

Contents

List of Figures

Chapter 1

Introduction

Achromatic holographic lithography (AHL) is a method of producing fine period gratings over large areas. Such structures are of interest in a number of applications including atomic interferometry, optoelectronics, spectroscopy, and quantum effect electronics. They will be especially useful as a fiducial reference for fabricating large area devices such as high density DRAMS.

Currently fine period gratings are produced using electron beam lithography or using coherent holographic lithography. However, electron beams are not practical for producing a grating over a large area, and conventional holographic lithography cannot produce grating periods smaller than $200\,nm$ due to the lack of a coherent laser source with wavelengths smaller than $351\,nm$. AHL is a way of using a partially coherent, short wavelength laser source and a parent grating to produce a grating with one half the period. With proper alignment, the grating can be produced over arbitrarily large areas. The challenge with performing AHL reliably is aligning the optics within a tight depth of focus budget.

At MIT AHL is now used to fabricate $100\,nm$ period gratings. The apparatus at MIT was designed by Anthony Yen[1] and later refined by Dan Olster[2]. This thesis discusses my work to improve the depth of focus alignment using a white light interferometer.

Chapter 2

Theory

2.1 Conventional Holography

Conventional holographic lithography is done by splitting coherent radiation and recombining the beams on a photosensitive surface. The holography equation which describes this phenomenon is

$$\Lambda = \frac{\lambda}{2sin\theta} \tag{2.1}$$

Where λ is the wavelength of the light and Λ is the period of the standing wave which the light produces. From this equation it is clear that for a given λ, it is impossible to produce gratings finer than $\lambda/2$. Because of the lack of coherent laser sources below $351\,nm$, conventional holography cannot be used to produce $100\,nm$ gratings.

A diagram of the setup used for holographic lithography is shown in Figure 2-1. The purpose of the pockels cell is to correct for environmental effects including vibration and warm air currents. Such disturbances may change the effective path length of one of the interfering beams on the order of $\lambda/4$. This would shift the standing wave on the substrate and significantly lower the contrast during a long exposure. The pockels cell provides a closed loop by varying its index of refraction to stabilize the interference pattern on the substrate.

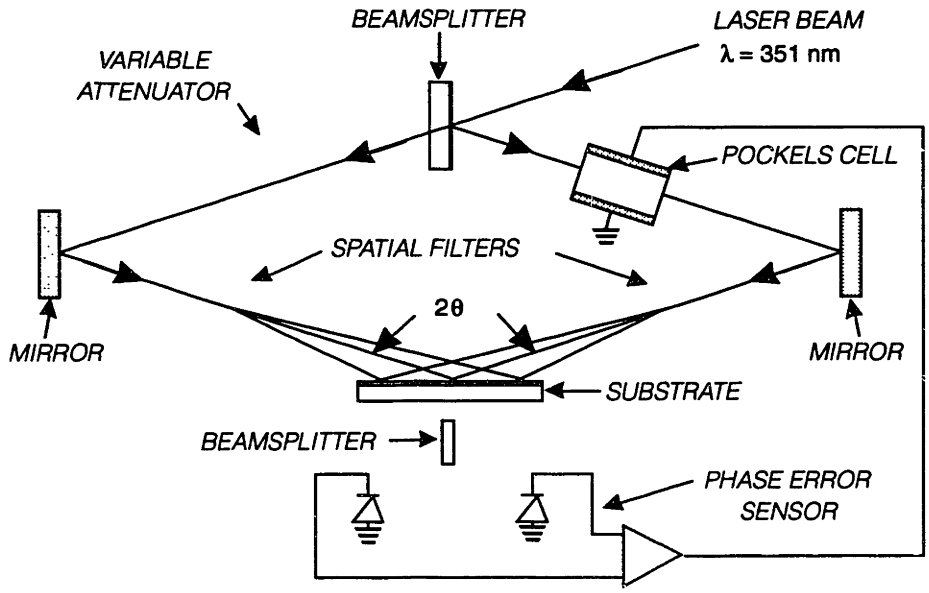

Figure 2-1: Schematic of holographic lithography

2.2 Achromatic Holography

Achromatic holographic lithography makes it possible to produce gratings of period Λ using only partially coherent radiation with $\lambda \leq 2\Lambda$. AHL uses radiation to image a parent grating instead of imaging the radiation.

This technique becomes clear by looking at an example taken from microscopy. We want to image an object containing spatial frequency Λ as seen in the diagram below

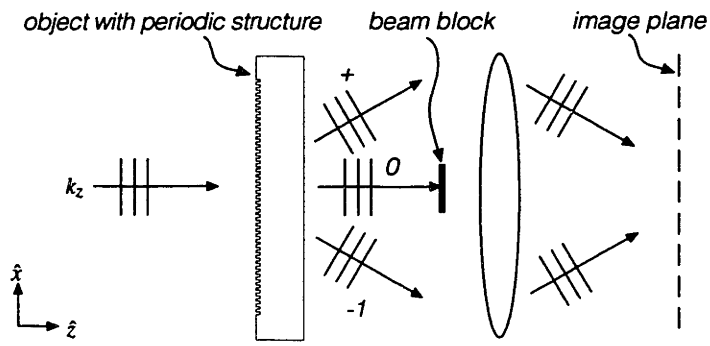

Figure 2-2: Imaging an object of spatial frequency k_z

Assume the illumination is a plane wave represented by

$$E(x,y,z) = Ae^{j(k_x x + k_y y + k_z z - \omega t + \phi)} \tag{2.2}$$

At the object plane we set z=0. The field in this plane is

$$E(x,y,z)\,|_{z=0} = Ae^{j(\phi - \omega t)} \tag{2.3}$$

If this radiation is used to image an object containing spatial frequency Λ, the light will diffract. We will make the assumption that the only existing diffracted orders are 0, +1, and -1. Recalling the diffraction equation,

$$m\lambda f = \sin\theta_{out} - \sin\theta_{in} \tag{2.4}$$

We see from this equation that the assumption that the +- 1 orders exist requires that the wavelength of the source is shorter than 2Λ. After diffracting off the object, we block the zero order beam using an opaque object, and the expression for the diffracted beams (ignoring the phase offset ϕ) are

$$E_{-1}(x) = \epsilon e^{j(-k_x x - \omega t)} \tag{2.5}$$

and

$$E_{-1}(x) = \epsilon e^{j(-k_x x - \omega t)} \tag{2.6}$$

where the factor of ϵ accounts for the first order grating efficiency. This light may be focused using a lens. In the image plane of the lens, the two beams interfere and the the intensity distribution is given by

$$I(x) = (E_{+1}(x) + E_{-1}(x))(E_{+1}(x) + E_{-1}(x))^* \tag{2.7}$$

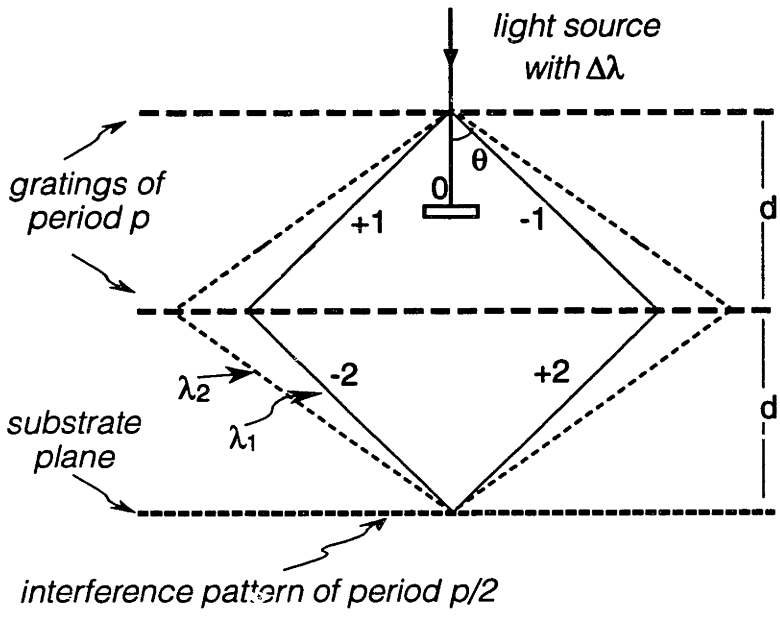

Figure 2-3: Diagram of achromatic holographic lithography

$$I(x) = 2 \mid \epsilon \mid^2 (1 + \cos 2k_x x) \tag{2.8}$$

The standing wave in this expression is an artifact from the fact that the illumination on the object is a plane wave. The period of the standing wave is half the period in the object which created it, and it is independent of the wavelength of the source. Achromatic holographic lithography takes advantage of this artifact to expose a fine period grating in the interference pattern as in the diagram in Figure 2-3.

2.3 Requirements for AHL

In the example given above, we assumed a coherent, planar light source. In reality, it is possible to use a partially coherent laser source. The incoherence of the source will result in multiple standing waves in the image plane. These waves will have identical period but different phases which results in diminished contrast. To quantify this, we first state that the condition for grating contrast is when the error in phase between the multiple standing waves is less than $\pi/2$. If the illumination has spatial divergence $\Delta\theta$, then the condition for

grating contrast, as calculated by A. Yen, is

$$\Delta d = \frac{\sqrt{p^2 - \lambda^2}}{2\Delta\theta} \tag{2.9}$$

where Δd is the difference in path length between interfering beams. This figure of merit is called the "depth of focus" since it requires that the substrate is focused properly in the image plane of the gratings.

2.4 Importance of working within the Depth of Focus

An analysis by Scott Hector shows that the depth of focus condition is critical for exposing high contrast gratings over large areas. High contrast and large area are features necessary for making AHL a practical technology.

For the general case of interference of two plane waves with intensities I_1 and I_2,

$$I(x) = I_1 + I_2 + 2\sqrt{I_1 I_2}\Gamma\cos[()x] \tag{2.10}$$

The parameter Γ is called the degree of mutual coherence. Its value ranges between 0 and 1.0 with 1.0 representing a perfectly coherent source. Γ considers both spatial and temporal coherence, but because AHL is achromatic only spatial coherence is considered. This paper does not compute Γ for the AHL configuration. Following from Equation 2.10,

$$Imin = I_1 + I_2 - 2\sqrt{I_1 I_2}\Gamma \tag{2.11}$$

$$Imax = I_1 + I_2 + 2\sqrt{I_1 I_2}\Gamma \tag{2.12}$$

Define γ, the differential development rate to be

$$\gamma = \left(\frac{I_{max}}{I_{min}}\right)^3 \tag{2.13}$$

The parameter γ describes the difference in development rate between the grating lines and

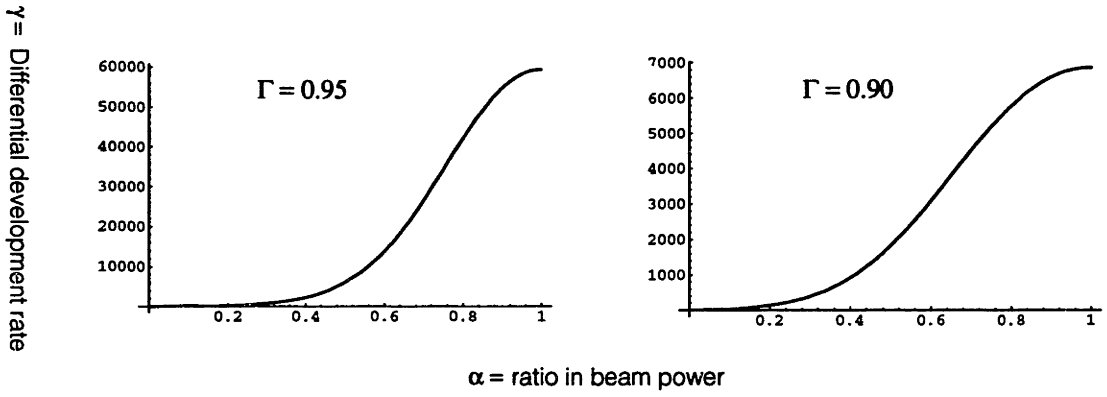

Figure 2-4: Development rate versus beam intensity ratio for two values of spatial coherence, showing a strong dependence of grating contrast on coherence.

spaces. The cubic dependence considers the response of the particular resist and developer (PMMA and MIBK) in our implementation of AHL. It is desirable to maximize γ in order to obtain vertical grating sidewalls, and to be able to control the linewidth easily.

Define a parameter α to be the ratio in beam power between the two arms. In AHL, α depends on the blazing of the parent gratings and on the angle of incidence of the light source on the parent grating.

$$\alpha \equiv \frac{I_1}{I_2} \tag{2.14}$$

Then the equation for differential development rate as a function of contrast and intensity balancing is

$$\gamma = \left(\frac{1 + \alpha + 2\sqrt{\alpha}\Gamma}{1 + \alpha - 2\sqrt{\alpha}\Gamma} \right)^3 \tag{2.15}$$

As seen the plots in Figure 2-4, γ depends strongly on Γ and weakly on α. This emphasizes the importance of working AHL within a tight depth of focus budget.

Chapter 3

Apparatus

The apparatus for AHL in the Submicron Structures Laboratory at MIT is set up to produce $100\,nm$ gratings. The parent gratings consist of $200\,nm$ period holographically fabricated gratings etched in plates of fused quartz (Suprasil). The quartz plates are $3.5\,in$ in diameter and $0.5\,in$ thick. Suprasil, the type of quartz used for the plates, has an index of refraction of 1.46 throughout the visible range. Using a Michelson interferometer, A. Yen selected the quartz plates to vary less than $0.5\,\mu m$ in thickness from one another in order to use mechanical spacers to align the gaps.

The laser source is an old Lumonics ArF ($\lambda = 193\,nm$) excimer laser rated at 10 watts. Its beam is elliptical in shape measuring $2.5\,cm$ horizontally and $0.5\,cm$ vertically near the front of the laser. The horizontal divergence is $6\,mrad$ and the vertical divergence is $2\,mrad$. The beam is rotated with mirrors to take advantage of the lower vertical divergence for AHL.

The lithography is done in poly methyl methacrylate (PMMA) on an anti-reflection coating (ARC) developed by A. Yen specifically for $193\,nm$. The ARC and PMMA are spun and baked on a four inch silicon wafer which is held flat with a vacuum pinchuck behind the parent gratings. The developer used is an IPA/MIBK solution. The lithography process is explained in detail in D. Olster's thesis.

In A. Yen's original setup, scotch tape ($100\,\mu m$ thick) was used as a mechanical spacer

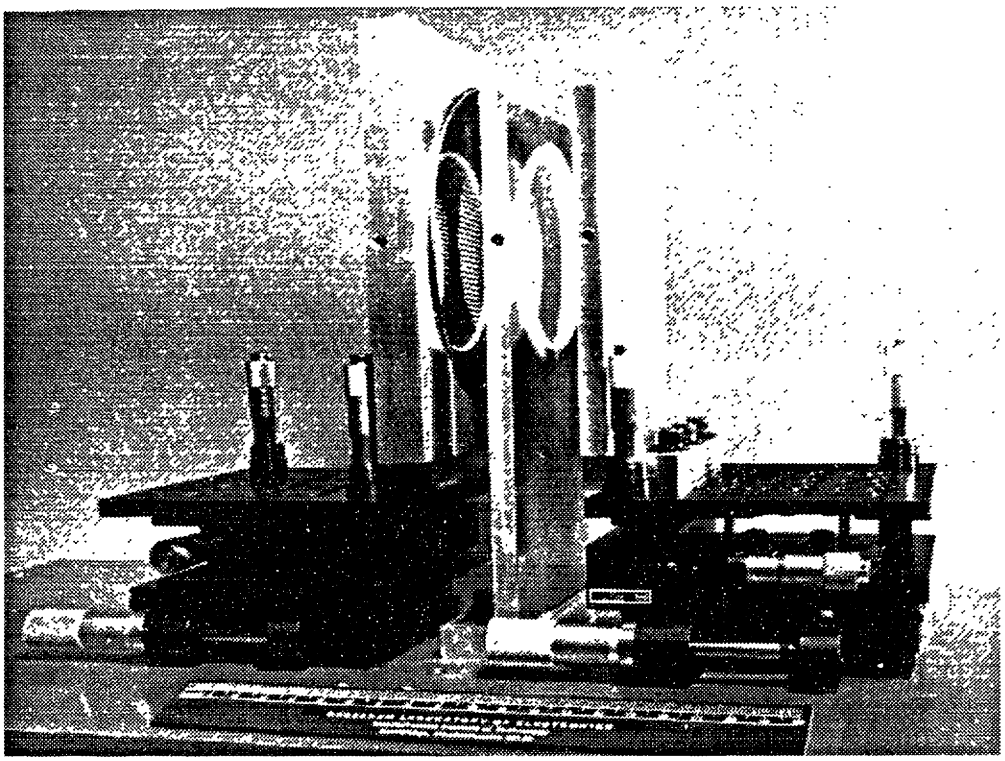

Figure 3-1: Photograph of the AHL setup at MIT. The quartz plates with $200\,nm$ period gratings and the silicon pinchuck are mounted vertically. The gaps between them are adjusted using the micrometer bases.

to set equal gaps between the front plate and the back plate and the substrate. Shortly before I began working on the apparatus, D. Olster began to use optical fibers as the spacer of choice because of its superior uniformity.

Chapter 4

The White Light Interferometer

4.1 Motivation

We determined that mechanical spacers are not a reliable way to bring the system within the depth of focus. One problem is that the silicon substrate may not be flat between the point of contact of the spacers and the area to be exposed. Another problem is potential damage mechanical spacers could do to the AHL optics, especially if thin membranes are to be used as the substrate. We also felt that mechanical spacing is a crude method of alignment for an optical setup.

4.2 White Light Paths

The original idea is to shine a beam a white light through the AHL optics as shown in Figure 4-1. Given that A. Yen used a Michelson interferometer to match the thicknesses of the quartz plates to $0.5\,\mu m$, then the beams at point B will interfere with highest contrast when the two gaps are exactly equal. The four beams shown in Figure 4-1b have similar paths to the beams of interest, but if the polarization of the white light is normal to the plane of incidence, they will not interfere with the interferometer because every beam in air undergoes a phase shift of π as it reflects off a dielectric such as quartz or the silicon substrate. Therefore if the thicknesses of the plates are matched, the four beams will

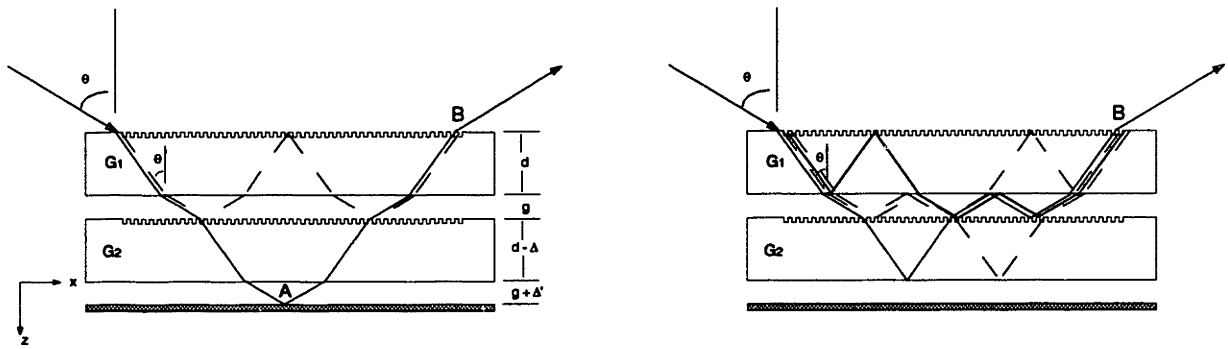

Figure 4-1: Paths of interfering white light beams. The figure on the left shows the paths of the beams of interest which will interfere at B. The figure on the right shows extraneous beams which will diminish the interference contrast if the plates are not of equal thicknesses.

destructively interfere and their power goes back to the source.

4.3 Light source

The white light source for this application must have low temporal coherence and high spatial coherence. If the temporal coherence is too long, then the beams of interest will interfere strongly when the substrate is out of focus by multiples of $d\lambda$ where d depends on the angle of incidence of the light on the substrate. If the coherence length is extremely short, then the beams will interfere if and only if the system is in focus. A low coherence length is synonymous to a broadband source, so a hot incandescent source is desirable.

If the spatial coherence is too low, then the beams will diverge and become lost in background noise. Hence the light source must be collimated and have a small source size.

We considered using sunlight because of its good collimation and broad spectrum, but it was not available in the lab where the apparatus was set up. The source we used is a fiber-light with collimating optics, as shown in Figure 4-2. The first fine slit lowers the effective source size in the plane of the interfering beams. The collimating lens we selected is a laser collimator which has a short focal length and a high numeric aperture creating an intense, collimated beam when a point source is placed at its focal point. Aligning the

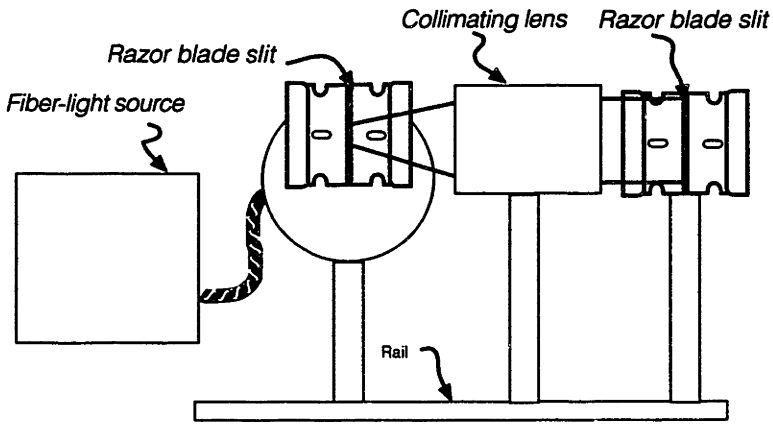

Figure 4-2: Setup of collimated white light source. The first slit shrinks the source size. The second slit acts as a simple aperture.

collimating lens is done by reflecting the collimated beam back through the lens. The light should focus back onto the source.

4.4 Setting up the Interferometer

In order to have the highest fringe contrast, the beams of interest must have equal intensities. The ratio of the power in the beams is determined by the reflectivity R at the air-quartz and air-substrate boundaries seen in Figure 4-1. The equation governing R is

$$R = \left(\frac{\sin(\theta_{air} - \theta_{quartz})}{\sin(\theta_{air} + \theta_{quartz})} \right)^2 \tag{4.1}$$

where θ_{air} and θ_{quartz} describe the path of the excimer beam in the gaps and plates and are related by Snell's law. Suprasil, the quartz used in the plates, has an index of 1.46 for visible light, and the index of the substrate is somewhat higher so it is at least as reflective as the quartz. To meet the condition of equal beam intensity, $R = 0.5$ and $\theta_{air} = 79.4^o$.

If maximum interference contrast is not critical, then θ_{quartz} can also be determined

to follow the path of the excimer beam more closely. This method can compensate for differences in thickness between the quartz plates. The angle of incidence of the excimer beam traveling through the quartz plates if given by

$$m\lambda f = n \sin \theta_{quartz} - \sin \theta_{air} \tag{4.2}$$

For normal incidence of the excimer beam on the front grating, $\theta_{air} = 0^o$ and $\theta_{quartz} = 42^o$. Fortunately, this angle is very close to the 44^o angle giving highest contrast in the white light interference pattern. This cooincidence makes it possible to use quartz plates of arbitrary thickness in the apparatus.

4.5 Setting up the Detector

The beams of white light in the plane of the detector display the pattern seen in Figure 4-3. The clusters of extraneous stripes on the left represent the various paths the white light can take as it travels through the plates and gaps. The separation of these beams on the screen is due to the different walks, or lateral offsets, of the beams, i.e. beams traveling through a $200\,\mu m$ gap at 79^o incidence will walk approximately $1.03\,mm$, and beams traveling through $0.5\,in$ plates at 44^o incidence will walk $12.4\,mm$. Since the walk in the plates is much larger than the walk in the gaps, the different clusters of beams represent different numbers of passes through the quartz plates.

An amplified photodiode monitors the intensity of the interfering beams. In order to filter the signal from the noise, the detector output is passed through a lock-in amplifier. A lock-in amplifier takes as its two inputs a signal and a reference frequency, and its output is the DC component of the convolution of the two inputs. This output is basically the strength of the component of the input signal at the reference frequency. The device is set up in this experiment as follows: an ordinary function generator creates a sinusoidal output at, say, $17\,Hz$. Using a high-voltage amplifier and a piezoelectric micrometer, the size of one of the gaps is varied at $17\,Hz$. If the time average of the gap sizes are equal then

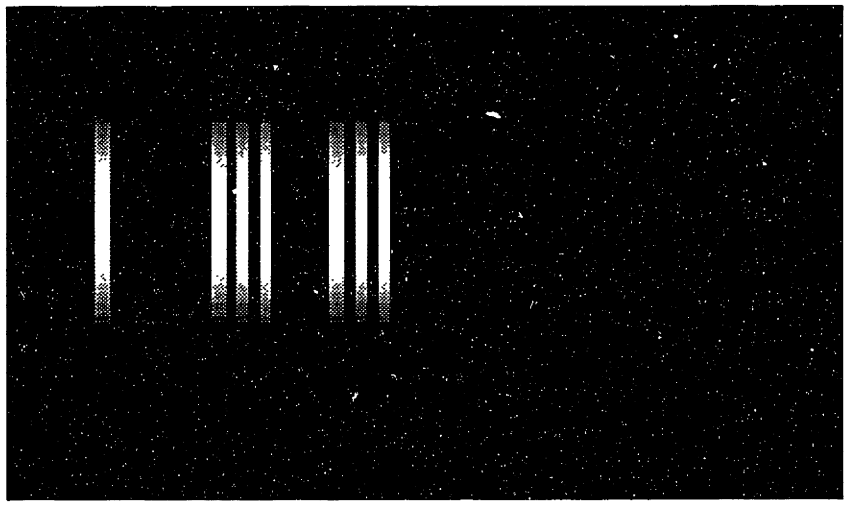

Figure 4-3: Pattern seen on a screen placed in the plane of the detector. The rightmost stripe shows interference when the apparatus is in alignment.

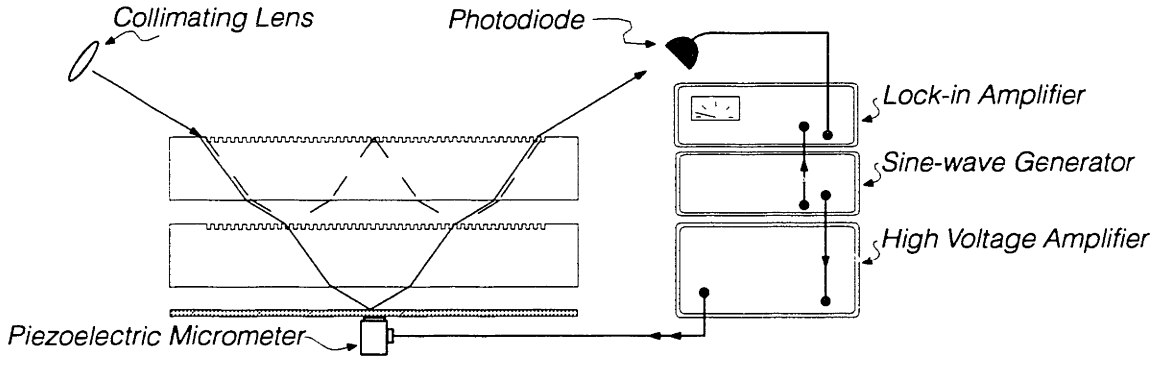

Figure 4-4: Interferometer detector scheme using a lock-in amplifier to monitor fringe contrast.

the condition for highest fringe contrast is met and the output of the lock-in amplifier is a maximum.

Chapter 5

Results

5.1 White Light Interference

Diagram 5-1 shows the signal taken from the photodiode with an oscilloscope for different amounts of swing in the piezo voltage. When the gap is properly aligned and the amplitude of the oscillation of the piezo is longer than the coherence length of the light source, the output from the detector is similar to the intensity pattern in a Michelson interferometer. When the swing in gap size is much smaller than a wavelength, the detector output is sinusoidal except for distortion caused by hysteresis in the piezo. The signal-to-noise ratio is good enough that the alignment can be done by eye with an oscilloscope instead of the lock-in amplifier.

Because of the steep 79.4^o angle of incidence, the length of the path the light takes through the second gap is approximately ten times the size of the gap. Hence the resolution of this interferometer is $\lambda/10$, or 50 nanometers. This precision is orders of magnitude better than what mechanical spacers could achieve.

5.2 Exposure Results

Using the new interferometer alignment, we were able to produce high contrast gratings up to $1\,cm^2$ as seen if Figure 5-2.

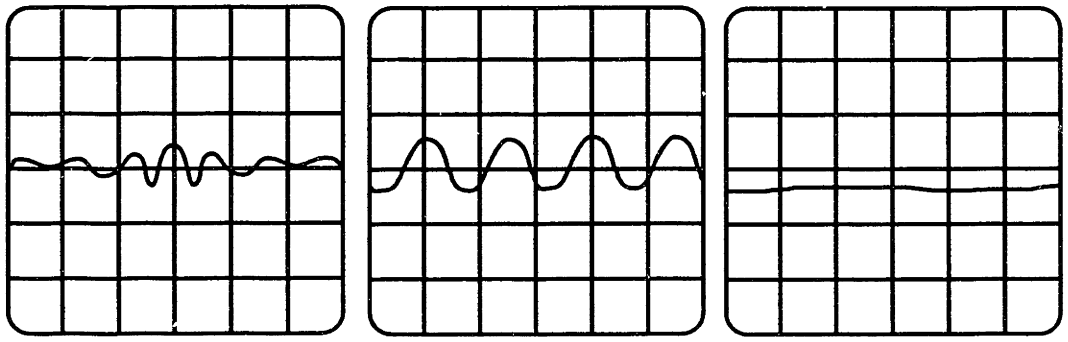

Figure 5-1: Oscilloscope displays of photodiode signals for large, small, and zero swing in piezo voltages.

5.3 Gap sizing

Results were repeatable for several gap sizes. A comfortable gap to work with is about $250\,\mu m$. Larger gaps are preferable since they give more flexibility in mounting the substrate, and they would make it easier to mechanically sweep the zero order stop to make large area gratings. The difficulty with larger gaps is that the walk of beams begins to exceed the diameter of the quartz plates and they walk off the edge of the plates.

5.4 Vibration

One concern with the new alignment scheme is the loss of the stability provided by mechanical spacers. In the current setup, the quartz plates and substrate are free to sway like a flagpole on their adjustable bases. Our results showed that this is not a serious problem, but it may become exacerbated in the future because longer exposure times during large area exposures would be more vibration prone, and mechanically sweeping the zero order stop may shake the apparatus.

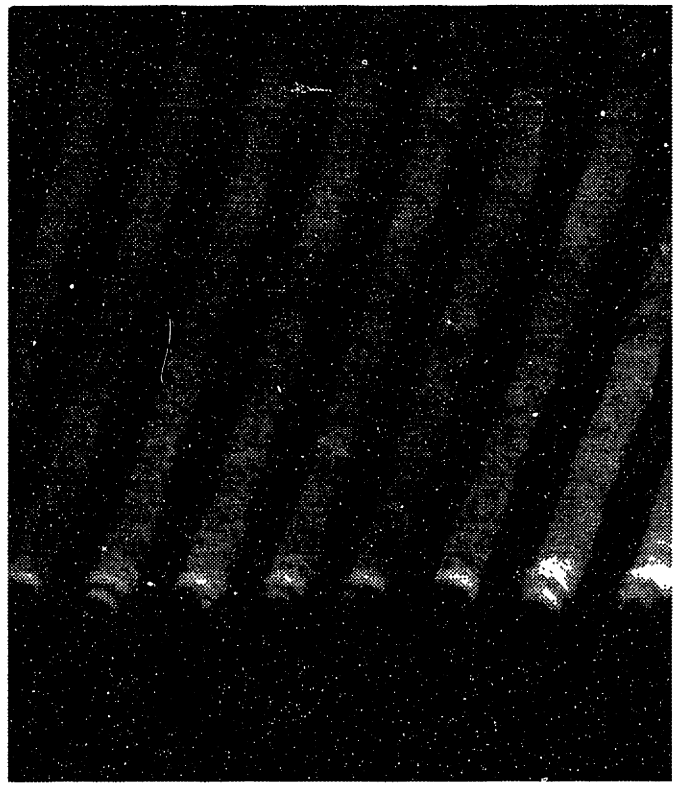

Figure 5-2: Scanning electron microscope photograph of 100 nm period gratings in PMMA.

Chapter 6

Future work

6.1 Changes to the setup

There is a need for better vibration control in the micrometer bases which are now in place. The bases will soon be replaced with mounts such as the one depicted in Figure 6-1. These will more rigidly hold the AHL optics.

The substrate holder will similarly be fitted with new micrometers, but the silicon pinchuck will also be replaced with an X-ray mask holder for exposing gratings directly on membranes and masks.

6.2 Changes to the optics

The technology for exposing $200\,nm$ period gratings holographically has improved greatly since when A. Yen fabricated the plates which are now used. New parent gratings should be made for AHL since the quality of the $100\,nm$ period gratings is totally dependent on the quality of the $200\,nm$ period gratings. To simplify the matter, the thicknesses of the new quartz plates do not have to be matched because of the new interferometer.

The excimer beam will be collimated using a cylindrical lens. Such a lens will both decrease the spatial incoherence of the beam and increase the intensity of the beam.

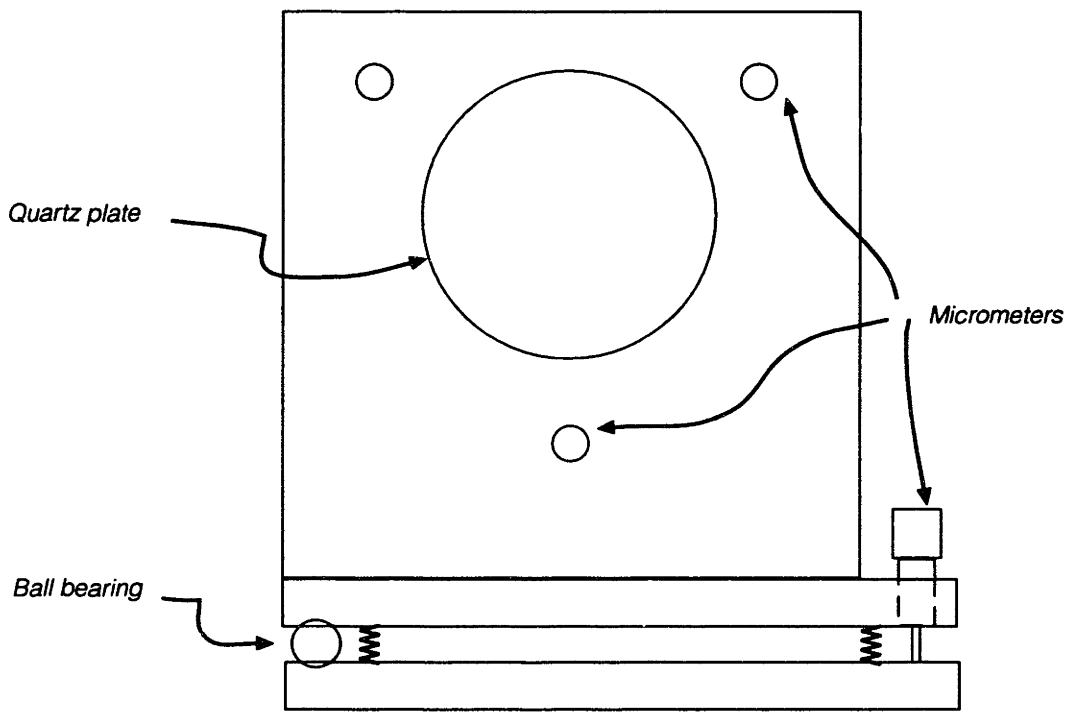

Figure 6-1: New holder for the front parent grating. Three micrometers adjust the spacing and parallelism of the plates, and one micrometer adjusts the parallelism of the grating lines.

6.3 Follow up work

Eventually we will produce free standing $100\,nm$ gratings on silicon nitride (Si_3N_4). The process for creating such structures is described in A. Yen's thesis. The gratings must be free standing for atomic interferometry research.

A. Yen proposed using AHL iteratively to produce $50\,nm$ period gratings once large area $100\,nm$ period gratings are available. Since the radiation source must have $\lambda \leq 100\,nm$, the lithography will have to be run using an undulator ($\lambda = 14$ nm) or plasma X-ray source.

Bibliography

[1] Anthony Yen. *Fabrication of Large-Area 100 nm-Period Gratings Using Achromatic Holographic Lithography.* PhD thesis, MIT, 1991.

[2] Dan Olster. *Refining the Process of Achromatic Holographic Lithography.* B.S. Thesis, MIT, Cambridge, MA, 1992.